Mechanism of Energy Transfer and Improvement Moist Stability of $BaMgAl_{10}O_{17}:Eu^{2+}$, Mn^{2+} Phosphor

Ru-Shi Liu and Wei-Chih Ke*

Department of Chemistry, National Taiwan University, Taipei 106, Taiwan
TEL:+886-2-3366-1169, e-mail: rsliu@ntu.edu.tw

Keywords: Phosphor, LED, BAM

Abstract

$BaMgAl_{10}O_{17}$ (BAM) co-doped with Eu^{2+} and Mn^{2+} was synthesized in a solid-state reaction and their luminescence properties were investigated as functions of the concentrations of the sensitizer and activator. BAM:Eu^{2+} had a broad blue emission band at 450 nm and BAM:Mn^{2+} exhibited green emission at 514 nm. The energy transfer from Eu^{2+} to Mn^{2+} was mainly of the resonance-type via an electric dipole-quadrupole interaction. Additionally, the addition of various fluxes such as AlF_3 and BaF_2 in the synthesis improves the moist and thermal stability. This is particularly important for the phosphor in white light emitting diodes (LEDs).

1. Introduction

White light-emitting diodes (LEDs) are regarded as the next-generation light source because of their high efficiency, weak environmental impact, long lifetimes, absence of mercury, short response times, applicability in final products of various sizes, and many more favorable properties. [1] Many methods are commonly applied to generate white light. The blue LED that coated with yellow phosphor is simpler and more widely used. However, the method faces serious problems of patent issue, poor color retention and high color temperature. Another approach is to use UV LEDs fitted with three phosphors emitting blue, red and green, this type offers superior color uniformity with a high color rendering index and excellent quality of light.

$BaMgAl_{10}O_{17}:Eu^{2+}$ and $BaMgAl_{10}O_{17}:Mn^{2+}$ are used as commercial blue and green phosphors for plasma display panels because of their high VUV efficiency. [2] The excitation spectrum of the blue BAM:Eu^{2+} had a broad absorption feature in the range 210-410 nm. Hence, BAM is expected to play an important role as the fluorescent material for UV LEDs. The spectral overlap between the excitation of the BAM:Mn^{2+} and the emission of the BAM:Eu^{2+} supports the expectation of effective energy transfer from Eu^{2+} to Mn^{2+} in the co-doped phosphor. [3] In the present work, $BaMgAl_{10}O_{17}$ (BAM) co-doped with Eu^{2+} and Mn^{2+} were synthesized in a solid-state reaction and their luminescence properties, energy transfer, and critical distance (R_c) were investigated. The BAM:$Eu_{0.15}$, $Mn_{0.3}$ with various fluxes was prepared and the influence of the fluxes on the luminescence, moist and thermal stability were examined. These properties are particularly important for phosphor in white light emitting diodes (LEDs).

2. Experimental

A series of BAM:$Eu_{0.15}$, Mn_y (y = 0-0.5) compounds were prepared by the solid state reaction method. The precursors $BaCO_3$, MgO, Al_2O_3, Eu_2O_3, and a trace amount of a specific flux such as AlF_3, BaF_2 or H_3BO_3 were weighed in stoichiometric amounts. Subsequently, mixture was mixed and ground together in an agate mortar. The powder products were then transferred into crucibles and fired at 1600°C in a 5% H_2/95% N_2 reducing atmosphere for 12 h. After firing, the samples were cooled to room temperature in the furnace, ground again into powders, and washed in deionized water

several times for further use. The composition and phase purity of the products were examined by synchrotron X-ray diffraction (XRD) using a large Debye-Scherrer camera that was installed at the BL01C2 beam line of National Synchrotron Radiation Research Center (NSRRC) with λ = 0.7749 Å, The photoluminescence (PL) of the samples was measured using a FluoroMax-3 & FluoroMax-P. Thermal quenching and activation energy were studied using a heating apparatus (THMS-600) in combination with PL equipment. The morphology of phosphors was analyzed using a Hitachi S2400 electron microscope.

3. Results and discussion

XRD patterns of the BAM:$Eu_{0.15}$, Mn_y (y = 0-0.5), which match those of pure $BaMgAl_{10}O_{17}$ phase (JCPDS 26-0163) with the β-alumina structure. Figure 1 plots experimental, calculated, and difference results of the XRD refinement of BAM:$Eu_{0.15}$, $Mn_{0.3}$. This crystallizes as an orthorhombic structure with a space group of $P6_3/mmc$ and lattice constants of $a = b = 5.6456(5)$ Å, $c = 22.7016(2)$ Å, and v (cell volume) = 626.633(10) $Å^3$. All of the observed peaks satisfy the reflection condition, $\chi^2 = 2.61$, $R_p = 5.31\%$, and $R_{wp} = 7.04\%$.

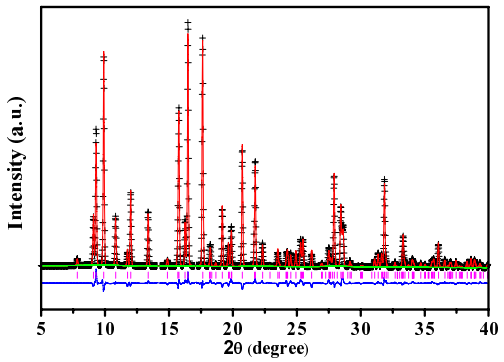

Fig. 1. XRD refinement of BAM:$Eu_{0.15}$, $Mn_{0.3}$.

Emission and excitation of BAM:Eu^{2+} occur through the 4*f*-5*d* transition. A broad excitation band was observed, matching closely that of the widely used near-UV LED chips. The 370 nm excitation produced a very strong emission band that peaked at 450 nm. The excitation spectrum of BAM:Mn^{2+} consists of four peaks around 360, 386, 427, and 452 nm, corresponding to the transitions from $^6A_1 \rightarrow {}^4T_2(^4D)$, $^6A_1 \rightarrow (^4A_1,{}^4E)(^4G)$, $^6A_1 \rightarrow {}^4T_2(^4G)$, and $^6A_1 \rightarrow {}^4T_1(^4G)$ in the 3*d* levels of Mn^{2+} ions, respectively. The 452 nm excitation produced a broad emission band that peaked at 514 nm. The spectral overlap between the excitation of the activator (Mn^{2+}) and the emission of the sensitizer (Eu^{2+}), effective energy transfer from Eu^{2+} to Mn^{2+} is expected in the co-doped phosphor. Figure 2 shows the PL and PLE spectra of Eu^{2+} and Mn^{2+} co-doped BAM:$Eu_{0.15}$, Mn_y phosphors with various dopant contents y of 0-0.5 with the fixed Eu^{2+} concentration at 0.15. The excitation spectrum shows a broad band, which corresponds to the 4*f*-5*d* transition of Eu^{2+} ions, implying this phosphor can be well excited by NUV light. The intensities of the emission from Eu^{2+} decrease and those from Mn^{2+} increase.

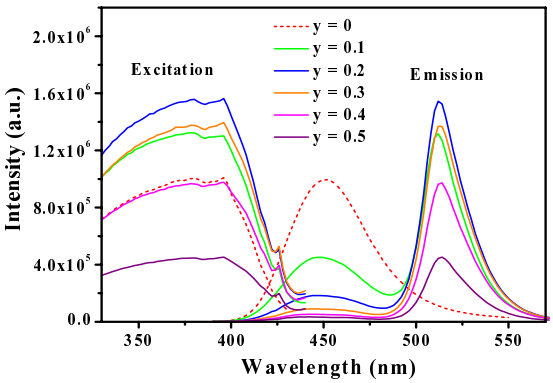

Fig. 2. Excitation and Emission spectra of BAM:$Eu_{0.15}$, Mn_y (y = 0-0.5). (excited at 370 nm)

Based on Förster and Dexter's energy transfer formula of multi-polar interaction and Reisfeld's approximation, the following relation can be obtained. [4-6]

$$\frac{I_{S0}}{I_S} \propto C_{Eu+Mn}^{n/3}$$

where I_{S0} is the intrinsic luminescence intensity of Eu^{2+} and I_S is the luminescence intensity of Eu^{2+} in the presence of the Mn^{2+}; C is the sum of the contents of Eu^{2+} and Mn^{2+}; and n = 6, 8, and 10, corresponding to dipole–dipole, dipole–quadrupole, and quadrupole–quadrupole interactions. The nature of the interaction in the transfer process can be determined by plotting I_{S0}/I_S vs $C_{Eu\text{-}Mn}^{n/3}$, as in Figure 3a and b; a linear relationship is observed only when n = 8. This result clearly indicates that the energy transfer from Eu^{2+} to Mn^{2+} is the dipole-quadrupole mechanism, which is expected to be the dominant mode due to the parity allowed transition of Eu^{2+} and the parity non-allowed transitions of Mn^{2+}.

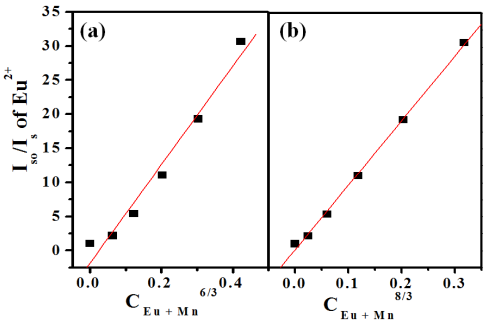

Fig. 3. Dependence of I_{so}/I_s of Eu^{2+} on (a) $C_{Eu\text{-}Mn}^{6/3}$ and (b) $C_{Eu\text{-}Mn}^{8/3}$.

The transfer probability of *d-d* and *d-q* interactions is given by Förster. [4,6] For the dipole-quadrupole mechanism, the critical distance (R_c) of energy transfer from Eu^{2+} to Mn^{2+} can be found using eq.

$$R_c^8 = 0.63\times10^{28}\frac{f_q\lambda_S^2 Q_A}{f_d E_S^4}\int F_S(E)F_A(E)dE$$

where $Q_A = 4.8\times10^{-16}$ f_d $cm^2\cdot eV$ is the integrated absorption cross-section of the activator (Mn^{2+}); $f_d = 10^{-7}$ and $f_q = 10^{-10}$ are the oscillation strengths of the electric dipole and quadrupole transitions for Mn^{2+}; λ_S = 4500 Å and E = 2.8 eV are the emission wavelength and emission energy of Eu^{2+}, and $\int F_S(E)F_A(E)dE$ represents the spectral overlap between the normalized shapes of the Eu^{2+} emission $F_S(E)$ and Mn^{2+} excitation $F_A(E)$, and is estimated at about 1.83 eV^{-1}. Accordingly, the critical distance for energy transfer was calculated to be about 10.9 Å.

Flux is generally employed to improve the quality of phosphors. [7-9] Figure 4 shows the PL spectra of BAM:$Eu_{0.15}$, $Mn_{0.3}$ with various fluxes and the relative intensity and CIE coordinates are listed in Table 1. The fluxes significantly enhance the luminescence intensity and color saturation. Therefore, the synthesized with AlF_3 has a higher relative emission intensity (116%) compare than commercial phosphor and higher color purity.

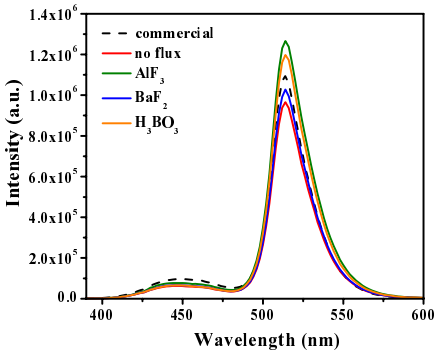

Fig. 4. PL spectra of BAM:$Eu_{0.15}$, $Mn_{0.3}$ with various fluxes. (excited at 370 nm)

Table 1. Relative intensity and CIE coordinates of BAM:$Eu_{0.15}$, $Mn_{0.3}$ with various fluxes.

Flux	*emission (nm)*	*Relative intensity*	*CIE x*	*CIE y*
commercial	514	100	0.1292	0.5832
no flux	514	88	0.1338	0.6214
AlF_3	514	116	0.1355	0.6302
BaF_2	514	94	0.1329	0.6226
H_3BO_3	514	109	0.1337	0.6412

Figure 5 shows the SEM morphology of BAM:$Eu_{0.15}$, $Mn_{0.3}$ with various fluxes. In general, BAM phosphor has a plate-shaped morphology due to its crystallographic characteristics. The phosphor particles with a fluoride base flux have a hexagonal surface morphology. A sample prepared by H_3BO_3 flux is semispherical and not smooth. The results also show that the morphology of phosphor particles affects their luminous property and stability.

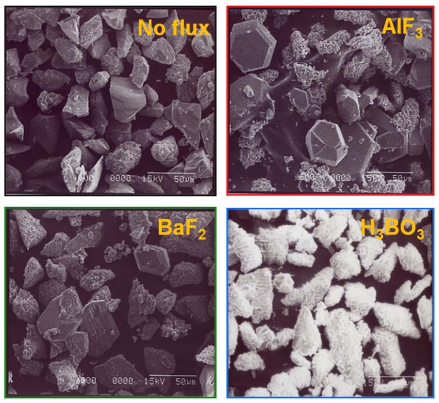

Fig. 5. SEM image of BAM:$Eu_{0.15}$, $Mn_{0.3}$ with various fluxes.

Figure 6 depicts the thermal quenching of the luminescence spectra of BAM:$Eu_{0.15}$, $Mn_{0.3}$ at various temperatures from 25°C to 300°C. The decrease in the emission intensity and the corresponding FWHM (Full Width at Half Maximum) were obtained, which can be assigned to thermal quenching at configurationally coordinate diagram. [10,11] The inset plots the temperature dependent relative emission intensity of BAM:$Eu_{0.15}$, $Mn_{0.3}$ with various fluxes and commercial YAG:Ce^{3+}. In particular, synthesis with fluxes such as AlF_3 can enhance the thermal quenching temperature (T_{50}), all the samples have a higher T_{50} than a commercial YAG:Ce^{3+}, with values of over 300°C, indicating superior thermal stability as a luminescent material for white LEDs.

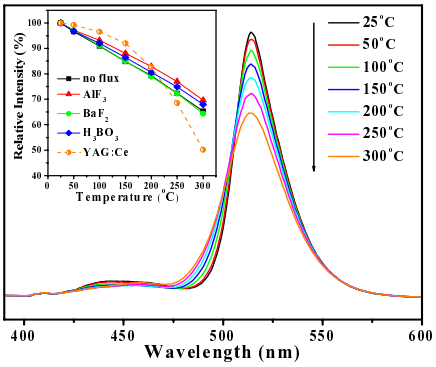

Fig. 6. Temperature dependence of emission spectra of BAM:$Eu_{0.15}$, $Mn_{0.3}$. Inset shows temperature-dependent relative emission intensity of samples with various fluxes and YAG:Ce^{3+}.

Moist Stability is one of the important technological parameter for phosphors used in white LEDs. In this work, the measurement of conductivity as a function of time has been used. Figure 7 plots the measurements for BAM:$Eu_{0.15}$, $Mn_{0.3}$ with various fluxes. The increase in conductivity depends on time due to the interaction between moisture and host of phosphor, and fact that some ions of the phosphor host are dissolved in water. Especially, Synthesis with fluoride base fluxes such as AlF_3 and BaF_2 can enhance the moist stability. The result is obtained because the phosphor particles with a fluoride base flux, which have a highly crystalline hexagonal surface morphology, cannot interact easily with the moisture. However, the sample with H_3BO_3 as flux has lowest stability owing to the absence of high crystalline particles and smoothness surface. The PL spectra of as-received and hydrated for samples with AlF_3 and H_3BO_3 as fluxes indicate the approximate change in total integrated radiance is about −9% and −22%. Hence, synthesis with fluxes can enhance the moist stability, it is found that AlF_3 has better performance than BaF_2 or H_3BO_3.

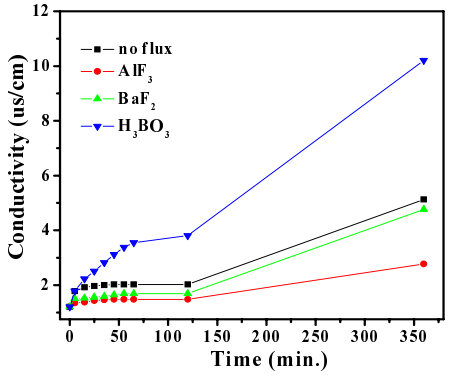

Fig. 7. Conductivity of BAM:$Eu_{0.15}$, $Mn_{0.3}$ as function of time with various fluxes.

4. Summary

$BaMgAl_{10}O_{17}$ co-doped with Eu^{2+} and Mn^{2+} was synthesized in a solid-state reaction. The energy transfer from Eu^{2+} to Mn^{2+} was mainly of the resonance-type via electric dipole-quadrupole interaction. The critical distance (R_c) was calculated of 10.9 Å. In addition, the addition of various fluxes such as AlF_3 and BaF_2 in the synthesis improved the moist and thermal stability. This was an important requirement for phosphor of white light emitting diodes (LEDs).

Acknowledgments

The authors would like to thank for the financial supports from the National Science Council (Contract nos. NSC 97-2113-M-002-012-MY3 and NSC 97-3114-M-002-005), the Economic Affair (Contract no. 97-EC-17-A-07-S1-043), Taiwan and the Chi Mei Corporation (Tainan, Taiwan).

5. References

1. Schubert, E. F.; Kim, J. K. *Science* **2005**, 308, 1274.
2. Zhang, J.; Zhang, Z.; Tang, Z.; Yao, Y.; Long, X. *Chem. Mater.* **2002**, 14, 3005.
3. Yang, P.; Yao, G. Q.; Lin, J. H. *Opt. Mater.* **2004,** 26, 327.
4. Förster , Th. *Ann. Physik.* **1948**, 2, 55.
5. Dexter, D. L.; Schulman, J. A. *J. Chem. Phys.* **1954**, 22, 1063.
6. Yang, W. J.; Luo, L.; Chen, T. M.; Wang, N. S. *Chem. Mater.* **2005,** 17, 3883.
7. Jung, K. Y.; Lee, H. W.; Kang, Y. C.; Park, S. B.; Yang, Y. S. *Chem. Mater.* **2005,** 17, 2729.
8. Deng, C. Y.; He, D. W.; Zhuang, W. D.; Wang, Y. S.; Kang, K.; Huang, X. W. *Chin. phys.* **2004**, 13, 473.
9. Rao, R. P. *J. Electrochem. Soc.* **2005**, 152, H115.
10. Shionoya, S.; Yen, W. M. *Phosphor Handbook*, Laser & Optical Science & Technology Series (CRC, New York, 1998), pp. 65-220.
11. Kim, J. S.; Park, Y. H.; Kim, S. H.; Choi, J. C.; Park, H. L. *Solid State Comm.* **2005,** 133, 445.